Millimeter-Wave Tapered-Slot Antennas on Synthesized Low Permittivity Substrates

Jeremy B. Muldavin, *Student Member, IEEE,* and Gabriel M. Rebeiz, *Fellow, IEEE*

***Abstract*—This paper presents 30-GHz linear-tapered slot antennas (LTSA) and 94-GHz constant-width slot antennas (CSWA) on synthesized low dielectric constant substrates ($\epsilon_r = 2.2$). The performance of tapered-slot antennas (TSA) is sensitive to the effective thickness of the substrate. We have reduced the effective thickness by selectively machining holes in the dielectric substrate. The machined substrate antenna radiation patterns were significantly improved independent of the machined hole size or lattice as long as the quasi-static effective thickness remained the same, even if the hole/lattice geometry is comparable to a wavelength. The method was applied at 94 GHz on a CSWA with excellent radiation pattern improvement, making it suitable for f/1.6 imaging array applications.**

***Index Terms*— Artificial substrates, micromachining, tapered-slot antennas.**

I. Introduction

TAPERED-SLOT antennas (TSA's) have been developed by Gibson *et al.* [1] and Yngvesson *et al.* [2], [3] for phased-array and focal-plane imaging systems. The performance of a TSA is sensitive to the thickness and dielectric constant of the antenna substrate. An *effective thickness*, which represents the electrical thickness of the substrate, has been defined as $t_{eff} = t(\sqrt{\epsilon_r} - 1)$. One accepted range of the effective thickness (determined experimentally) for good operation of a TSA is given as $0.005\lambda_o \leq t_{eff} \leq 0.03\lambda_o$ [2]. For substrate thickness above the upper bound of effective thickness, unwanted substrate modes develop that degrade the performance of the TSA, while antennas on thinner substrates suffer from decreased directivity.

The upper bound on the effective thickness $t_{eff} \leq 0.003\lambda_o$ necessitates mechanically thin substrates for millimeter-wave applications, even if low dielectric constant materials are used. For example, a maximum thickness of 200 μm (8 mils) is allowed for a 94-GHz TSA integrated on an $\epsilon_r = 2.2$ dielectric substrate. This results in a mechanically fragile substrate.

One way of improving the mechanical stability is to increase the thickness of the substrate and then selectively remove parts or nearly all of the underlying dielectric material. If nearly all of the substrate is removed, the TSA can be suspended on a thin dielectric membrane with an effective dielectric constant of $\epsilon_r = 1.05$ [4]. This is easily implemented at submillimeter-wave frequencies (300–3 THz), but is not as practical at millimeter-wave frequencies (30–300 GHz) since the membrane dimensions are large and the mechanical stability of the suspended membrane is compromised. Other researchers (Vowinkel *et al.* [5]) have selectively removed large portions of the dielectric inside the slot area of the TSA with good results.

Another method commonly used at millimeter-wave frequencies is the integration of the radiating antenna on a thin (4–8 mil) low dielectric substrate with $\epsilon_r = 2.2$ backed by a thick foam substrate with a dielectric constant of less than 1.1 [6], [7]. While this is excellent at 20–100 GHz, the thin dielectric substrate will interefere with the radiation patterns of TSAs at frequencies greater than 100 GHz. Therefore, it is advantageous to develop a technique to further reduce the dielectric constant of the dielectric support substrate.

In this work, an array of closely drilled holes is used to remove a portion of the underlying substrate, thereby resulting in a lower quasi-static (effective) dielectric constant substrate. This technique has been applied successfully using microstrip antennas [8]. The volume of the dielectric removed can be precisely controlled (between 0–100%) and determines the effective dielectric constant of the substrate. In this application, around 40–50% of the substrate is removed to maintain good mechanical properties.

II. 30-GHz Design and Measurements

A. LTSA Design

A nonoptimal linear TSA (LTSA) design, shown in Fig. 1, was chosen for the 30-GHz experiments. The LTSA was designed to be $4\lambda_o$ long with a 12° taper angle, which results in nearly one λ_o aperture. The slotline feed was 200–300 μm wide. The substrate is 1.27 mm (50 mils) thick RT/duriod, with a relative dielectric constant of $\epsilon_r = 2.2$. Three different substrates were investigated: *solid substrate*, *big hole substrate*, and *small hole substrate*. The big hole and small hole patterns, shown in Fig. 2, were machined in a 45° rotated rectangular lattice with an automated milling machine. The big hole substrate was chosen to be a large fraction of a wavelength with $D = \lambda_o/3$ (3.18 mm) and $W = \lambda_o/2$ (5.08 mm). The small hole pattern was chosen with $D = \lambda_o/8$ (1.27 mm) and $D = \lambda_o/5$ (2.03 mm). Previous measurements at 10 and 30 GHz have shown that the lattice choice (rectangular, hexagonal, etc.) has no effect on the far-field patterns for low dielectric constant substrates [9].

Manuscript received July 1, 1998; revised June 10, 1999.

The authors are with the Radiation Laboratory, Department of Electrical Engineering and Computer Science, University of Michigan, Ann Arbor, MI 48109 USA.

Publisher Item Identifier S 0018-926X(99)07972-7.

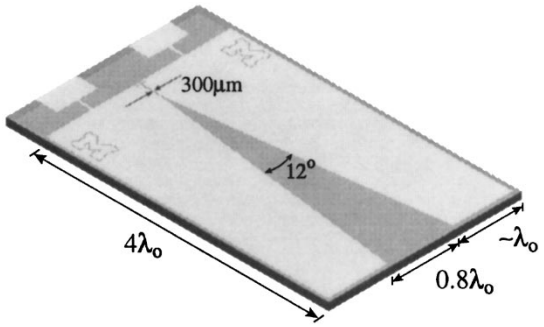

Fig. 1. The LTSA on a 1.27-mm-thick RT/durioid ($\epsilon_r = 2.2$) substrate. The pads on the end of the antenna are for low-frequency signal pickup.

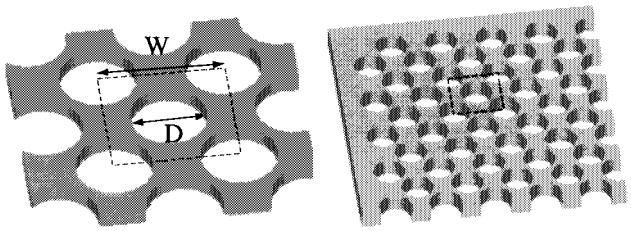

Fig. 2. Hole patterns machined into the substrates of the 30-GHz TSA's. The larger pattern has a hole diameter D of 3.18 mm (125 mils) and a spacing W of 5.08 mm (200 mils). The smaller pattern has a hole diameter of 1.27 mm (50 mils) and a spacing of 2.03 mm (80 mils). The dashed box represents the unit cell.

TABLE I
COMPARISON OF THE 3- AND 10-dB BEAMWIDTHS FOR THREE DIFFERENT 30-GHz TSA SUBSTRATES

Antenna	3-dB		10-dB	
	E-plane	H-plane	E-plane	H-plane
Solid substrate	17	54	66	67
Big/small hole	25	26	42	43

The machined substrates were chosen to have the same effective relative dielectric constant. The effective dielectric constant is a quasi-static value given by the volumetric average dielectric constant of the machined substrate and is $\epsilon_{\text{eff}} = (\pi/2)(D/W)^2 + \epsilon_r[1-(\pi/2)(D/W)^2]$, where D and W are defined in Fig. 2.

For RT/duroid, with $\epsilon_r = 2.2$, the effective dielectric constant ϵ_{eff} is equal to 1.46 for the two machined substrates shown in Fig. 2. For a 30-GHz TSA integrated on 1.27-mm (50 mils)-thick substrate, this reduction in the effective dielectric constant changes the value of t_{eff}/λ_o from 0.061 for the solid substrate to 0.026 for the machined substrates, placing the effective thickness just within the performance limits of Yngveson *et al.* [2].

B. 30-GHz Measurements

The normalized radiation patterns of the antennas were measured in an anechoic chamber. The thin leads and the pads on the slot end of the antenna (Fig. l) were designed to allow pickup of low frequency signals from a zero-bias Schottky diode (Metelics MSS20141-B10D, $C_t = 0.8$ pF) placed over the slot line of the antenna, one quarter of a guided wavelength from a capacitive RF short. The RF source

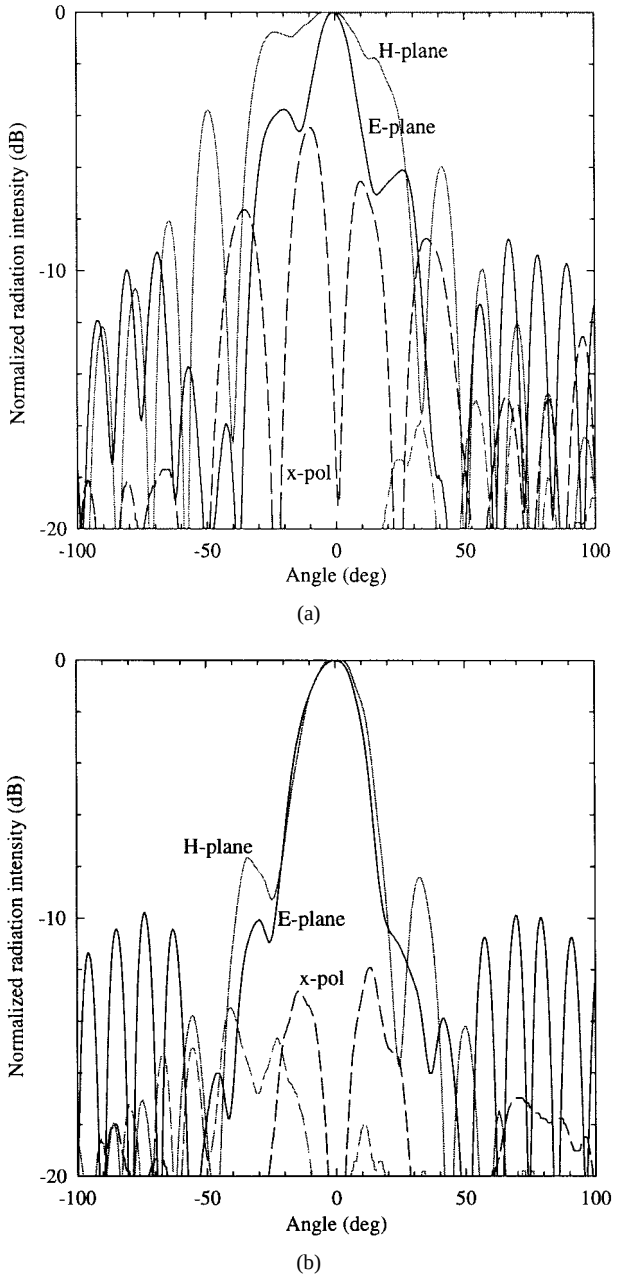

Fig. 3. Measured 30-GHz far-field antenna patterns for (a) the solid substrate and (b) the big hole LTSA.

was AM modulated at 5 kHz and radiated by a standard gain horn. The detected low-frequency signal (5 kHz) at the diode terminals was delivered to a lock-in amplifier. The amplified signal was then read by a computer, which controlled the antenna mount positioner.

The 30-GHz far-field radiation patterns of the solid substrate and the big hole substrate antennas are shown in Fig. 3. There was significant improvement in the far-field patterns of both the E- and H-plane with the machined substrates. Note the lower cross-polarization levels in the E- and H-plane patterns for the machined big hole antenna. No directivity values are quoted since the 45-plane copolarization and cross-polarization patterns were not measured. The big hole and the small hole TSAs gave very similar patterns to within $\pm$ 1° and $\pm$1 dB

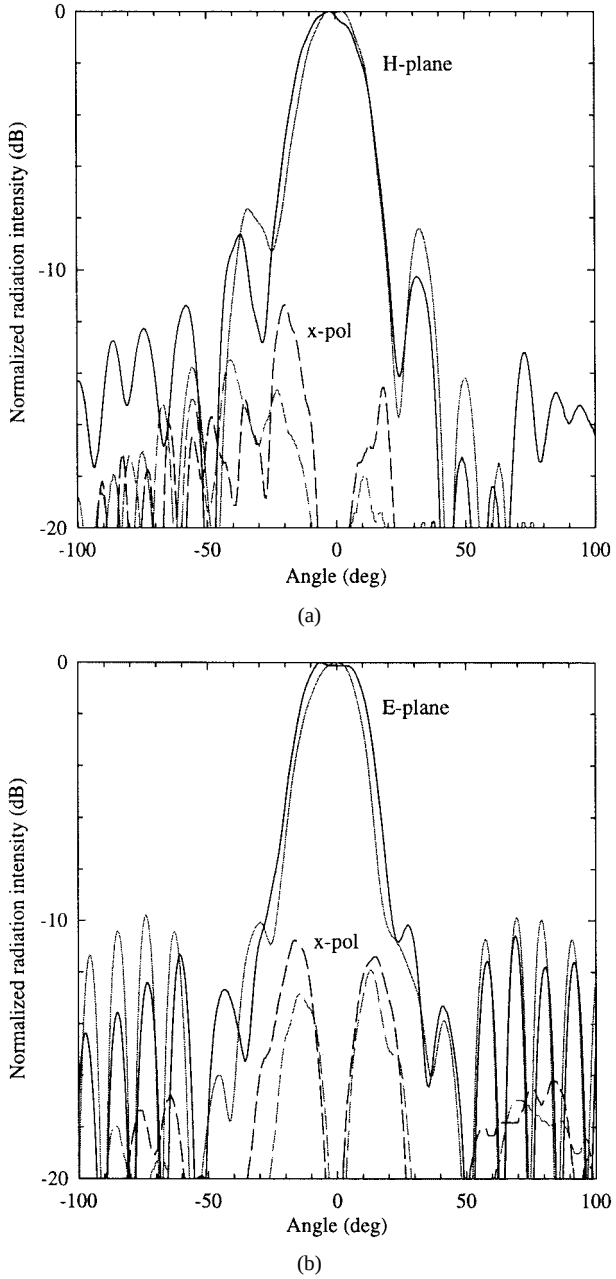

Fig. 4. Measured 30-GHz (a) H-plane and (b) E-plane far-field antenna patterns for the big hole (gray) and small hole LTSA (black).

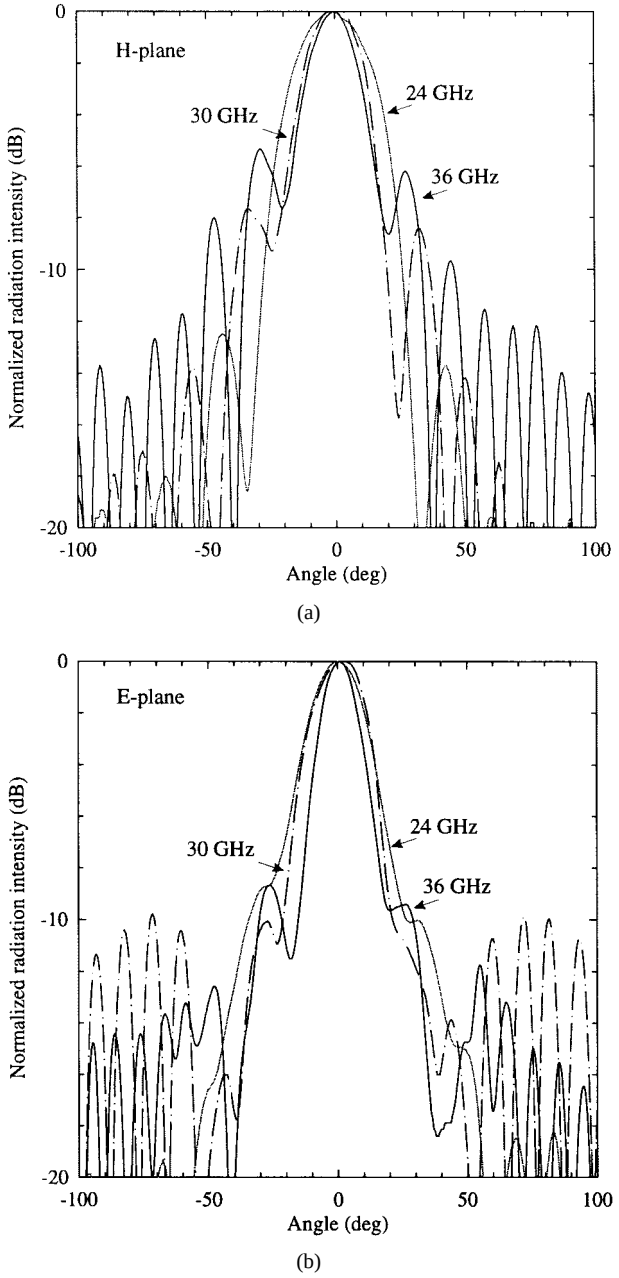

Fig. 5. Measured 24 (gray), 30 (dash-dot), and 36 GHz (solid): (a) H-plane and (b) E-plane far-field copolarization antenna patterns for the big hole LTSA.

(Fig. 4). This indicates that the improvement in performance is independent of hole geometry even if the holes/periods are a large fraction of a wavelength. This further suggests that the effect is purely a quasi-static reduction of the substrate dielectric constant and not a mode-suppression/photonic bandgap mechanism typically seen in high-dielectric constant substrates [10].

The 3- and 10-dB beamwidths for all three antennas are summarized in Table I. Notice the fine structure (or ripple) in the measured patterns at angles above $\pm 40°$. This is believed to be an interference pattern from the measurement setup and the edge of the TSA substrate. Recently, Sugawara *et al.* have shown that TSA patterns are very sensitive to currents induced on the edge of the finite-width substrate. These edge currents are in opposite phase to the slot-antenna currents and result in interference-like patterns at large measurement angles [11]. The big hole antenna results in symmetrical patterns at 30 GHz and for a 10-dB taper in an imaging lens system, the antenna will fit an $f/1.25$ lens.

A comparison of the measured 24-, 30-, and 36-GHz far-field radiation patterns for the big hole antenna is shown in Fig. 5. The backside radiation patterns ($|\theta| \geq 90°$) were below -15 dB. The peak cross-polarization levels were below -12.5, -10.5, and -8.5 dB at 24, 30, and 36 GHz, respectively. The corresponding patterns of the small hole LTSA are virtually identical and are not shown. As the frequency increases, the beamwidth decreases, the sidelobe levels increase, and the patterns degrade as the effective thickness increases (as

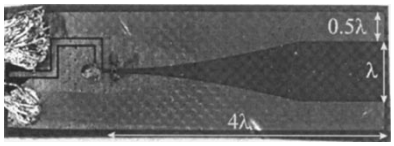

(a)

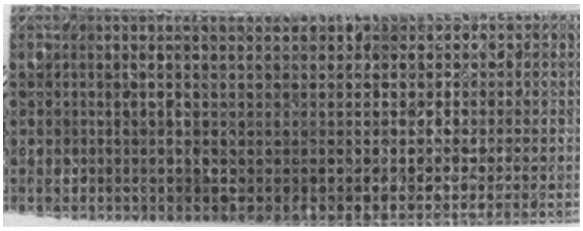

(b)

Fig. 6. (a) Front-side conductor pattern and (b) back-side hole pattern for the CWSA 94-GHz antenna. The antenna aperture is approximately λ_o, and the length is approximately $4\lambda_o$. The hole diameter is 380 μm and the unit cell width is 610 μm.

expected). Note that even at 36 GHz with $D = \lambda_o/2.5$ and $W = \lambda_o/1.6$, the big hole TSA gave virtually identical patterns to the small hole TSA with $D = \lambda_o/6.3$ and $W = \lambda_o/4$.

III. 94 GHz Design and Measurements

A. 94-GHz Design

A constant width TSA design, provided by Dr. E. Moore, Millimetrix Corporation, was used for the 94-GHz experiments (Fig. 6). In order to obtain an effective thickness of $t_{\text{eff}} \leq 0.03\lambda_o$ at 94 GHz, the solid substrate thickness must be less than 200 μm, resulting in a mechanically unstable substrate. Increasing the thickness to 380 μm (15 mils) improves the mechanical stability to a practical level. We compared 380-μm-thick solid substrate antennas to antennas machined with a hole pattern, shown in Fig. 2, having a diameter of 380 μm ($\lambda_o/9$) and a spacing of 610 μm ($\lambda_o/5$). In retrospect, these dimensions were chosen to be unnecessarily small and can easily be enlarged by a factor or two to three. The machining removes approximately 40% of the substrate and again results in an effective dielectric constant of 1.46. The effective thickness of the antenna is reduced from 0.058 to 0.025, again just within the acceptable limits.

B. 94-GHz Measurements

The 94-GHz measurements were performed on a bench top with absorber placed around the perimeter of the bench. The measurements were performed with an experimental setup similar to the 30-GHz setup except with an AM modulated 94-GHz Gunn diode source. An alpha diode (DMK2784-000, $C_t = 0.04$ pF) placed across the slot was used to detect the modulated signal. A SNR of greater than 20 dB was achieved.

The 94-GHz far field antenna patterns for the solid substrate and the machined CWSA are shown in Fig. 7. The CWSA showed excellent pattern improvement for the machined case, with low cross-polarization levels (-13 dB). The sharp -10 dB sidelobes are believed to be due to the edge currents on the finite width ($0.5\lambda_o$) conductor half plane. The machined CWSA results in an average -10 dB beamwidth of 35° and fits an $f/1.6$ lens imaging system. It is expected that the antenna patterns will change when placed in a 2-D imaging array, and this is subject to current investigation in our group.

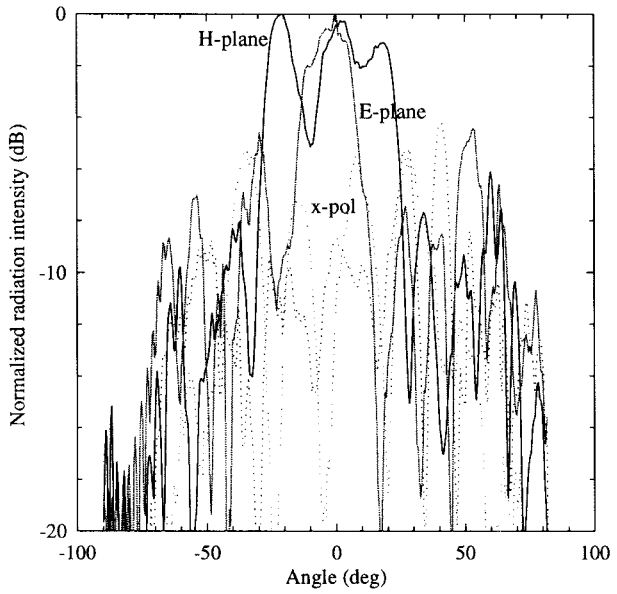

(a)

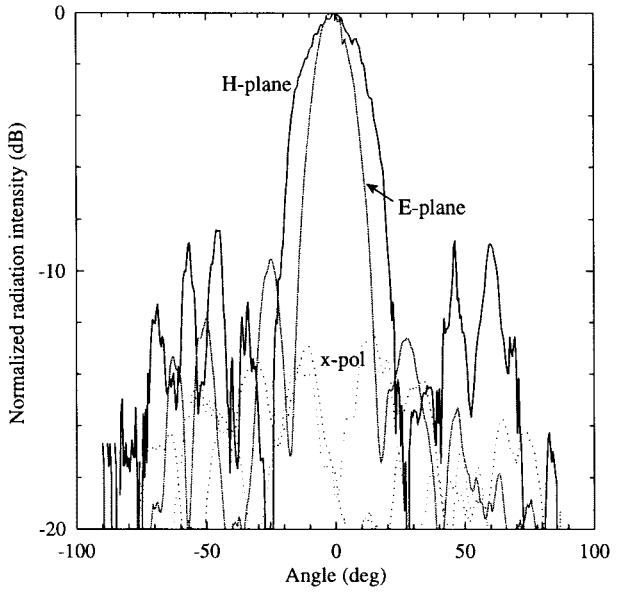

(b)

Fig. 7. Measured 94-GHz solid (a) substrate and (b) machined substrate antenna far-field CSWA patterns.

IV. Conclusions

We have shown that selective machining of a thick dielectric substrate results in a simple method for reducing the effective thickness of TSA's. In contrast to earlier measurements on high-dielectric constant substrates, if low-dielectric constant substrates are used, the improved far-field radiation patterns are not sensitive to hole geometry or lattice choice (as long as the quasi-static effective thickness remains the same) and can

be easily scaled with frequency from 10 to 94 GHz. A 94-GHz constant width TSA on a thick machined substrate ($\epsilon_r = 2.2$) was successfully fabricated, showing mechanical stability and practical radiation performance for imaging array applications.

REFERENCES

[1] P. J. Gibson, "The Vivaldi aerial," in *Proc. 9th Eur. Microwave Conf.*, Brighton, U.K., June 1979, pp. 101–105.

[2] K. S. Yngvesson, "Endfire tapered slot antennas on dielectric substrates," *IEEE Trans. Antennas Propogat.*, vol. 33, pp. 1392–1400, Dec. 1985.

[3] K. S. Yngvesson, T. L. Korzeniowski, Y. S. Kim, E. L. Kollberg, and J. F. Johansson, ,"The tapered slot antenna—A new integrated element for millimeter-wave applications," *IEEE Trans. Microwave Theory Tech.*, vol. 37, pp. 365–374, Feb. 1989.

[4] P. R. Acharya, H. Ekstrom, S. S. Gearhart, S. Jacobsson, J. F. Johansson, E. L. Kollberg, and G. M. Rebeiz, "The tapered slot antennas at 802 GHz," *IEEE Trans. Microwave Theory Tech.*, vol. 41, pp. 1715–1719, Oct. 1993.

[5] U. K. Kotthaus and B. Vowinkel, "Investigation of planar antennas for submillimeter receivers," *IEEE Trans. Microwave Theory Tech.*, vol. 37, pp. 375–380, Feb. 1989.

[6] G. P. Gauthier, A. Courtay, and G. M. Rebiez, "Microstrip antennas on synthesized low dielectric-constant substrates," *IEEE Trans. Antennas Propogat.*, vol. 45, pp. 1310–1314, Aug. 1997.

[7] J. F. Zürcher, "The SSFIP—A global concept for high performance broadband planar antennas," *Electron. Lett.*, vol. 24, no. 23, pp. 1433–1435, Nov. 1988.

[8] B. Zürcher, J.-F. Zürcher, and F. Gardiol, "Broadband microstrip radiators: The SSFIP concept," *Electromagn.*, vol. 9, pp. 385–393, Nov. 1988.

[9] T. J. Ellis and G. M. Rebiez, "millimeter-wave tapered slot antennas on micromachined photonic bandgap dielectrics," in *IEEE-MTT Int. Microwave Symp.*, San Francisco, CA, June 1996, pp. 1157–1160.

[10] ———, "Improvements in tapered slot antennas on thick dielectric substrates," in *IEEE Int. Symp. Antennas Propagat.*, Baltimore, MD, July 1996, pp. 992–995.

[11] S. Sugawara, Y. Maita, K. Adachi, K. Mori, and K. Mizuno, "Characteristics of a millimeter-wave tapered slot antenna with corrugated edges," in *IEEE-MTT Int. Symp.*, Baltimore, MD, June 1998, pp. 533–536.

[12] D. B. Rutledge, D. P. Neikirk, D. P. Kasilingam, and K. J. Button, "Integrated-circuit antennas," in *Infrared and Millimeter Waves.* New York: Academic, 1983, vol. 10, ch. 1.

[13] D. M. Pozar, *Microwave Engineering.* Reading, MA: Addison-Wesley, 1990.

[14] T. M. Weller, L. P. B. Katehi, and G. M. Rebeiz, "High-performance microshield line components," *IEEE Trans. Microwave Theory Tech.*, vol. 43, pp. 534–543 Mar. 1995.

Jeremy B. Muldavin (S'96) received the B.S.E. degree in engineering physics from the University of Michigan, Ann Arbor, in 1996. He is currently working toward the Ph.D. degree in electrical engineering at the same university.

He was a Student Rresearcher for four years in the High-Energy Spin Physics Group, University of Michigan. His research interests are in development and characterization of novel micro electro-mechanical systems (MEMS) structures and interconnects for components and subsystems in wireless communication systems.

Gabriel M. Rebeiz (S'86–M'88–SM'93–F'97) received the Ph.D. degree in electrical engineering from the California Institute of Technology, Pasadena, in 1988.

He joined the faculty of the University of Michigan, Ann Arbor, in September 1988 and was promoted to Full Professor in 1998. He has held short Visiting Professorships at Chalmers University of Technology, Gothenburg, Sweden, Ecole Normale Superieur, Paris, France, and Tohoku University, Sendai, Japan. His research interests are in applying micromachining techniques and micro electro-mechanical systems (MEMS) for the development of novel components and subsystems for wireless communication systems. He is also interested in Si/GaAs RFIC design for receiver applications, and in the development of planar antennas and microwave/millimeter-wave front-end electronics for applications in millimeter-wave communication systems, automotive collision-avoidance sensors, monopulse tracking systems, and phased arrays.

Dr. Rebeiz received the National Science Foundation Presidential Young Investigator Award in April 1991 and the URSI International Isaac Koga Gold Medal Award for Outstanding International Research in August 1993. He also received the Research Excellence Award in April 1995 from the University of Michigan. Together with his students, he is the winner of Best Student Paper Awards at IEEE-MTT (1992, 1994, 1996, 1998, and 1999), and IEEE-AP (1992, 1995) and received the JINA'90 Best Paper Award. He received the Electrical Engineering and Computer Science (EECS) Department Teaching Award in October 1997, the College of Engineering Teaching Award in May 1998, and was selected by the students as the 1997–1998 Eta Kappa Nu EECS Professor of the Year. In June 1998 he received the Amoco Foundation Teaching Award, given yearly to one (or two) faculty members at the University of Michigan, for excellence in undergraduate teaching.